Research in Astronomy and Astrophysics

PAPER

Laboratory study of the formation of fullerene (from smaller to larger, C_{44} to C_{70})/anthracene cluster cations in the gas phase

RAA 2020 Vol. **20** No. **12**, 202(8pp) doi: 10.1088/1674-4527/20/12/202

http://www.raa-journal.org *http://iopscience.iop.org/raa*

***R**esearch in*
***A**stronomy and*
***A**strophysics*

Laboratory study of the formation of fullerene (from smaller to larger, C_{44} to C_{70})/anthracene cluster cations in the gas phase

De-Ping Zhang (张德萍)[1,2], Yuan-Yuan Yang (杨园园)[1,2,3], Xiao-Yi Hu (胡潇毅)[1,2,3] and Jun-Feng Zhen (甄军锋)[1,2]

[1] CAS Key Laboratory for Research in Galaxies and Cosmology, Department of Astronomy, University of Science and Technology of China, Hefei 230026, China; *dpzhang@ustc.edu.cn; jfzhen@ustc.edu.cn*
[2] School of Astronomy and Space Science, University of Science and Technology of China, Hefei 230026, China
[3] CAS Center for Excellence in Quantum Information and Quantum Physics, Hefei National Laboratory for Physical Sciences at the Microscale, and Department of Chemical Physics, University of Science and Technology of China, Hefei 230026, China

Received 2020 January 17; accepted 2020 June 15

Abstract The formation and evolution mechanism of fullerenes in the planetary nebula or in the interstellar medium are still not understood. Here, we present the study on the cluster formation and the relative reactivity of fullerene cations (from smaller to larger, C_{44} to C_{70}) with anthracene molecule ($C_{14}H_{10}$). The experiment is performed in an apparatus that combines a quadrupole ion trap with a time-of-flight mass spectrometer. By using a 355 nm laser beam to irradiate the trapped fullerenes cations (C_{60}^+ or C_{70}^+), smaller fullerene cations $C_{(60-2n)}^+$, $n = 1-8$ or $C_{(70-2m)}^+$, $m = 1-11$ are generated, respectively. Then reacting with anthracene molecules, series of fullerene/anthracene cluster cations are newly formed (e.g., $(C_{14}H_{10})C_{(60-2n)}^+$, $n = 1-8$ and $(C_{14}H_{10})C_{(70-2m)}^+$, $m = 1-11$), and slight difference of the reactivity within the smaller fullerene cations are observed. Nevertheless, smaller fullerenes show obviously higher reactivity when comparing to fullerene C_{60}^+ and C_{70}^+. A successive loss of C_2 fragments mechanism is suggested to account for the formation of smaller fullerene cations, which then undergo addition reaction with anthracene molecules to form the fullerene-anthracene cluster cations. It is found that the higher laser energy and longer irradiation time are key factors that affect the formation of smaller fullerene cations. This may indicate that in the strong radiation field environment (such as photon-dominated regions) in space, fullerenes are expected to follow the top-down evolution route, and then form small grain dust (e.g., clusters) through collision reaction with co-existing molecules, here, smaller PAHs.

Key words: astrochemistry — methods: laboratory — ultraviolet: ISM — ISM: molecules — molecular processes

1 INTRODUCTION

Polycyclic aromatic hydrocarbons (PAHs) are well recognized as an essential component of the interstellar medium (ISM) and may account for $\leq$15% of the interstellar carbons. They are observed via the infrared (IR) emission bands at 3.3, 6.2, 7.7, 8.6, 11.3 and 12.7 μm widespread throughout the Universe (Allamandola et al. 1989; Genzel et al. 1998; Sellgren 1984; Tielens 2008, 2013; Li 2020). A huge effort was undertaken in the past few decades to identify the carriers of those IR emission features, however, no specific PAH responsible for the IR emission features has been identified. By contrast, another important type of carbonaceous species, fullerenes (C_{60} and C_{70}) have been unambiguously observed in planetary nebula Tc1 via their IR emission spectra (Cami et al. 2010). After that, C_{60} has also been detected in reflection nebulae (Sellgren et al. 2010; Peeters et al. 2012; Boersma et al. 2012), protoplanetary nebulae (Zhang & Kwok 2011), R Coronae Borealis stars (García-Hernández et al. 2011), the peculiar binary XX Oph (Evans et al. 2012), young stellar objects (Roberts et al. 2012) and diffuse clouds (Berné et al. 2017). Recently, the proposal of C_{60}^+ as the carrier of two DIBs (9577 Å and 9632 Å) was confirmed

by the laboratory spectrum recorded in the gas phase (Campbell et al. 2015), which also revealed some weaker absorption features. The weak C_{60}^+ features were subsequently detected in astronomical spectra (Walker et al. 2016; Cordiner et al. 2019).

Since the first discovery of C_{60} in the gas phase by Kroto et al. (1985), the fullerene molecules have been the topic of extensive laboratory studies (see e.g. Böhme (2011, 2016); Linnartz et al. (2020) and references therein), which provide important knowledge on the possible formation and evolution routes of fullerenes in the Universe. For example, the laboratory work showed that C_{60} can be formed starting form the carbon-rich seeded gas via a bottom-up formation route (see e.g. Jäger et al. 2008). Meanwhile, the laboratory experiment revealed that C_{60} can be generated from UV radiation induced photochemical evolution of large PAHs (Zhen et al. 2014). This may be a possible top-down route formation of C_{60} in the interstellar environment. The very recent laboratory work suggested that C_{60} can undergo facile formation from shock heating and ion bombardment of circumstellar SiC grains (Bernal et al. 2019). García-Hernández et al. (2013) summarized and discussed the possible formation mechanisms of fullerene in evolved stars and in ISM in their IR spectroscopic study of C_{60}/anthracene adducts.

Fullerenes and their ions are highly active due to the unsaturated features, and thus they can easily react with other molecules (Petrie et al. 1992; Murata et al. 2001; Böhme 2016; Omont 2016). Fullerene/PAHs adducts are one family of the fullerene reaction products and are of astrochemical interest. It is known that fullerene/PAHs adducts are generated via the Diels−Alder cycloaddition reactions (Briggs & Miller 2006; Petrie & Bohme 2000; Cataldo et al. 2014; Zhen et al. 2019c). Meanwhile, anthracene ($C_{14}H_{10}$) is among the simple PAH molecules, whose reaction with C_{60} has received considerable attentions. For example, Cataldo et al. (2014) reported the sonochemical synthesis of monoanthracene adduct $(C_{14}H_{10})C_{60}$ and bis-anthracene adduct $(C_{14}H_{10})_2C_{60}$ with the precursors of C_{60} and anthracene dissolved in benzene. The same group also studied the IR spectra of these adducts by using Fourier transform IR spectroscopy. More importantly, it is found that the IR spectra of the C_{60}/anthracene adducts are similar to those of C_{60} and other unidentified IR emission bands recorded by astronomical observations (García-Hernández et al. 2013). Motivated by García-Hernández et al. (2013)'s work, the formation and photochemistry of (C_{60} and C_{70})/anthracene cluster cations in the gas phase were investigated in this laboratory (Zhen et al. 2019c). The fullerene/anthracene cluster cations are formed from $C_{56/58/60}^+$ or $C_{66/68/70}^+$ and neutral anthracene molecules via ion-molecule reactions. Upon irradiation by a 355 nm laser beam, the cluster cations dissociated into fullerene cations and neutral anthracene molecules. Besides, the experimental results showed that C_{60}^+ and C_{70}^+ have lower reactivity compared to their neighbor fullerene cations ($C_{56/58}^+$ and C_{68}^+).

It should be mentioned that Candian et al. (2019) reported a theoretical study of the stability and IR spectra of neutral and ionized fullerenes with a coverage from C_{44} to C_{70}. By comparing the theoretical IR spectra to the observed emission spectra of several planetary nebulae, the authors suggested the possible presence of smaller cages (44, 50 and 56 carbon atoms) in the astronomical objects. In this contribution, we present a laboratory study of the formation of cluster cations between fullerene cations (C_{44}^+ to C_{70}^+) and anthracene molecules, and investigate the reactivity of these fullerenes, especially the ones containing 44, 50 and 56 carbon atoms. In order to generate the interested fullerene cations, higher laser energy and longer irradiation time are used compared to our recent work (Zhen et al. 2019c). The experimental details are given in the following section. The results and discussions, and astronomical implications are presented in Section 3 and Section 4, respectively. Our conclusions follow in Section 5.

2 EXPERIMENTAL METHODS

The experiment was performed using the quadrupole ion trap and time-of-flight (QIT-TOF) mass spectrometry setup, which has been described in detail elsewhere (Zhen et al. 2019a,c). Briefly, the gas phase fullerene molecules (C_{60} or C_{70}) were prepared by heating their powder samples at a temperature of $\sim$ 613 K and then ionized by electrons ($\sim$ 82 eV) produced in an electron gun (Jordan, C-950). The interested fullerene cations are selected by using an ion gate and a quadrupole mass filter (Ardara, Quad-925mm-01) and then guided into the quadrupole ion trap (Jordan, C-1251). Another oven (used at room temperature) mounted under the quadrupole ion trap was used to vaporize the anthracene powder. The gas phase anthracene molecules effused continuously towards the center of the ion trap. Through the ion-molecule reactions between fullerene cations and anthracene molecules in the ion trap, fullerene/anthracene cluster cations were produced. The third harmonic output (355 nm) of a Nd:YAG laser (Spectra-Physics, INDI) was used to irradiate the fullerene cations and fullerene/anthracene cluster cations and induce the photochemistry process. At an appropriate timing, the ions were extracted from the ion trap and detected by a reflection TOF mass spectrometer (Jordan, D-850).

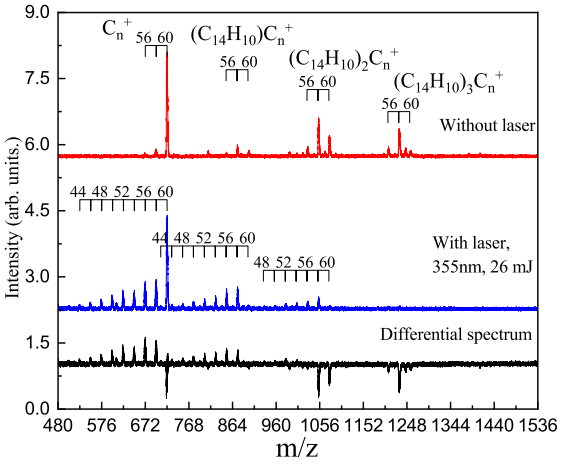

Fig. 1 Mass spectrum of fullerene (C_{60})/anthracene cluster cations recorded without laser irradiation (*top red trace*) and with laser irradiation (*middle blue trace*). We used 355 nm laser with energy of 26 mJ pulse^{-1} and irradiation time amounting to 1.6 s. The assignments of mass spectral peaks are shown. The differential spectrum between the blue trace (laser on) and the red trace (laser off) is also shown in the bottom trace with black color.

To produce smaller fullerenes, we optimized the experimental conditions and found that the laser energy and the irradiation time are critical to the production of smaller fullerene cations. By monitoring the intensity of new generated fragment ions in the mass spectrum, it is found that the optimal conditions are with the laser energy of $\sim$ 30 mJ pulse^{-1} and irradiation time of 1.6 s in each measured period.

The simple PAH, anthracene ($C_{14}H_{10}$), was used as the reactant to examine the reactivity of fullerene cations based on the following considerations. The fullerene/anthracene adducts are among the simple and typical fullerene/PAHs adducts. Therefore, the study of formation and photochemical processes of fullerene/anthracene adducts can provide a guidance for other fullerene/PAHs clusters. Furthermore, the anthracene molecule allows us to make a reasonable comparison with the previous work (Zhen et al. 2019c) where the same molecule is used as the reactant. In addition, due to its relatively high vapor pressure at room temperature, the anthracene molecule is suitable for our current experimental setup.

3 EXPERIMENTAL RESULTS AND DISCUSSIONS

The mass spectrum of the fullerene (C_{60})/anthracene cluster cations recorded without laser irradiation is shown in Figure 1 (top red trace). Fullerene cations ($C_{56/58/60}{}^+$) and series of fullerene/anthracene cluster cations ($(C_{14}H_{10})_nC_{56/58/60}{}^+$, $n = 1-3$) were produced in the experiment. The fullerene cations were generated by electron bombardment of neutral C_{60} molecules, and the cluster cations were formed via ion-molecule reactions between $C_{56/58/60}{}^+$ and anthracene molecules in the ion trap. Figure 1 (middle blue trace) shows the recorded mass spectrum of trapped fullerene/anthracene cluster cations after laser irradiation with energy of 26 mJ/pulse and irradiation time of 1.6 s (i.e., typically $\sim$16 pulses). It can be seen that series of fullerene cations ($C_{(60-2n)}{}^+$, n=0-8) and fullerene/anthracene cluster cations ($(C_{14}H_{10})C_{(60-2n)}{}^+$, n=0-8 and $(C_{14}H_{10})_2C_{(60-2n)}{}^+$, n=0-6) are formed in the ion trap. The bottom trace of Fig. 1 displays the differential spectrum to reflect the intensity changes of these cations formed under the conditions of laser-off and laser-on. It can be seen that the intensity of larger mass cluster cations ($(C_{14}H_{10})_{2/3}C_{56/58/60}{}^+$, $(C_{14}H_{10})C_{60}{}^+$) and fullerene cation ($C_{60}{}^+$) decreases after laser irradiation, while the intensity of other cations increases.

To clearly show the intensity changes, a zoom-in of the middle and bottom traces of Figure 1 is displayed in Figure 2. As the number of carbon atoms decreases, the intensities for fullerene cations, their mono-anthracene adducts and bis-anthracene adducts become weak gradually. Interestingly, the intensity of $(C_{14}H_{10})C_{60}{}^+$ is weaker not only than its neighbor ($(C_{14}H_{10})C_{58}{}^+$), but also than other smaller mono-adducts. Likewise, the intensity of $(C_{14}H_{10})_2C_{60}{}^+$ is weaker than the other smaller bis-adducts.

In recent study of Zhen et al. (2019c), laser energy of 1.3 mJ pulse^{-1} and irradiation time of 0.5 s were used to irradiate the trapped ions. The fullerene cations, $C_{56}{}^+$, $C_{58}{}^+$ and $C_{60}{}^+$, and their corresponding fullerene/anthracene cluster cations were recorded in the mass spectra (fig. 2 in Zhen et al. 2019c). By contrast, more smaller fullerene cations ($C_{(60-2n)}{}^+$, $n = 3-8$) and fullerene/anthracene cluster cations ($(C_{14}H_{10})C_{(60-2n)}{}^+$, $n = 3-8$ and $(C_{14}H_{10})_2C_{(60-2n)}{}^+$, $n = 3-6$) were newly observed in current mass spectra (Fig. 1). Note that the laser wavelength (355 nm) used in these two studies was the same. The newly observed smaller fullerene cations and their fullerene/anthracene cluster cations were due to the higher energy (26 mJ pulse^{-1}) and longer irradiation time (1.6 s) used in present experiment.

The observed smaller fullerene cations in present study (Fig. 1) all contain even numbers of carbon atoms, indicating the successive C_2 loss in the formation process, which has been known as the main evolution way followed by fullerene cations after absorption of photons (Lifshitz 2000; Zhen et al. 2014). Combining this consideration with previous studies (Zhen et al. 2014, 2019b,c), the following photochemistry mechanism (path 1–4) is suggested. After absorption of UV photons, fullerene/anthracene

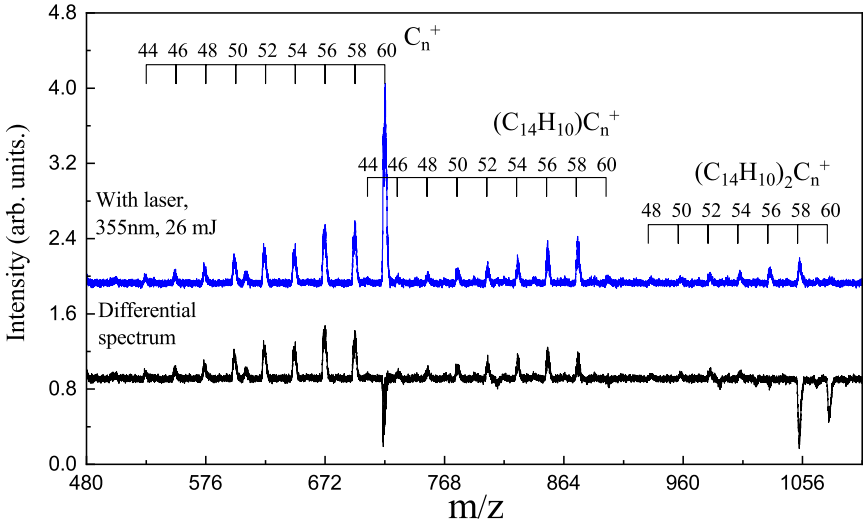

Fig. 2 The zoom-in mass spectrum of fullerene (C_{60})/anthracene cluster cations with laser irradiation and the differential spectrum in the range of m/z=480−1104.

cluster cations dissociated into fullerene cations and anthracene molecules (path 1). And then, the fullerene cations including free ones and ones resulted from the dissociation underwent successive C_2 loss and formed smaller fullerene cations (path 2). After that, the smaller fullerene cations reacted with anthracene molecules to form fullerene/anthracene cluster cations (path 3 and 4). The reaction pathways (in sequence) for the formed fullerene/anthracene cluster cations are summarized as below:

$$[(C_{14}H_{10})_{(1-3)}C_{56/58/60}]^+ \xrightarrow{h\nu} (C_{14}H_{10})_{(1-3)} + [C_{56/58/60}]^+ \quad (1)$$

$$[C_{56/58/60}]^+ \xrightarrow{h\nu} nC_2 + [C_{(60-2n)}]^+ \quad (2)$$

$$[C_{(60-2n)}]^+ + C_{14}H_{10} \longrightarrow [(C_{14}H_{10})C_{(60-2n)}]^+ \quad (3)$$

$$[(C_{14}H_{10})C_{(60-2n)}]^+ + C_{14}H_{10} \longrightarrow [(C_{14}H_{10})_2C_{(60-2n)}]^+ \quad (4)$$

In addition to C_{60}, C_{70} was also used as the precursor to produce the smaller fullerene cations and examine their reactivity with anthracene. The experiment conditions were same as those used for the study of C_{60} except for the laser energy of 30 mJ/pulse. The recorded mass spectra are depicted in Figure 3. The top red trace shows the mass spectrum of the C_{70}/anthracene cluster cations recorded without laser irradiation. Fullerene cations ($C_{68/70}{}^+$) and their anthracene cluster cations ($(C_{14}H_{10})_mC_{68/70}{}^+$, m=1,2 were observed. After irradiation of these trapped ions by the 355 nm laser beam with energy of 30 mJ/pulse and irradiation time of 1.6 s, the recorded mass spectrum is displayed as the middle blue trace in Figure 3. Series of fullerene cations ($C_{(70-2m)}{}^+$, $m = 2-11$), their mono-anthracene adducts ($(C_{14}H_{10})C_{(70-2m)}{}^+$, $m = 2-11$ and bis-anthracene adducts ($(C_{14}H_{10})_2C_{(70-2m)}{}^+$, $m = 2-9$) were newly formed comparing to the top trace without laser irradiation. To clearly show the changes in the mass spectra recorded without and with laser irradiation, the differential spectrum is derived by extraction the top trace (without laser beam) from the middle trace (with laser beam). The resultant spectrum is shown as the bottom trace in Figure 3. The peaks with positive intensity indicate that the cations were formed after laser irradiation, such as $C_{(70-2m)}{}^+$, m=2-11.

Figure 4 displays the zoom-in of the middle and bottom traces of Figure 3. It can be seen that the intensities for fullerene cations, their mono-anthracene adducts and bis-anthracene adducts became weak gradually as the carbon numbers get smaller. The intensity of $(C_{14}H_{10})C_{60}{}^+$ is weaker than its neighbors, $(C_{14}H_{10})C_{58}{}^+$ and $(C_{14}H_{10})C_{62}{}^+$. Likewise, the intensity of $(C_{14}H_{10})_2C_{60}{}^+$ is weaker than its neighbors, $(C_{14}H_{10})_2C_{58}{}^+$ and $(C_{14}H_{10})_2C_{62}{}^+$.

The increments in laser energy and irradiation time on the $C_{70}{}^+$/anthracene system resulted in the production of more smaller fullerene/anthracene cluster cations (see Fig. 3), which is similar as the $C_{60}{}^+$/anthracene system (Fig. 1). In the previous work (Zhen et al. 2019c), laser energy of 0.9 mJ/pulse and irradiation time of 0.5 s were used to irradiate the trapped $C_{70}{}^+$/anthracene cluster cations. The fullerene cations, $C_{70}{}^+$ and $C_{68}{}^+$, and their corresponding fullerene/anthracene cluster cations were recorded in the mass spectra (fig. 3 in Zhen et al. 2019c). Compared to those results, more smaller fullerene cations ($C_{(70-2m)}{}^+$, $m = 2-11$), their mono-anthracene adducts

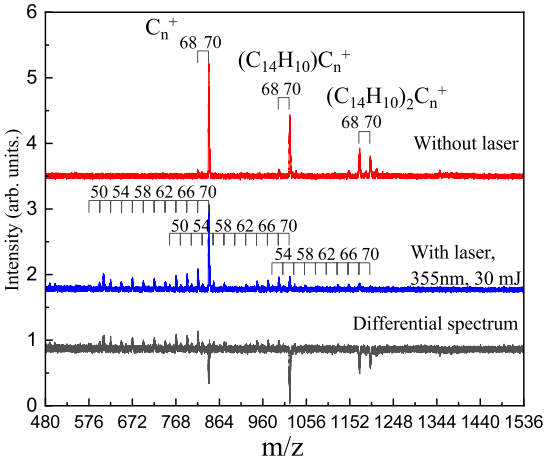

Fig. 3 Mass spectrum of fullerene (C_{70})/anthracene cluster cations recorded without laser irradiation (*top red trace*) and with laser irradiation (*middle blue trace*). We used 355 nm laser with energy of 30 mJ pulse^{-1} and irradiation time amounting to 1.6 s. The assignments of mass spectral peaks are shown. The differential spectrum between the blue trace (laser on) and the red trace (laser off) is also shown in the bottom trace with black color.

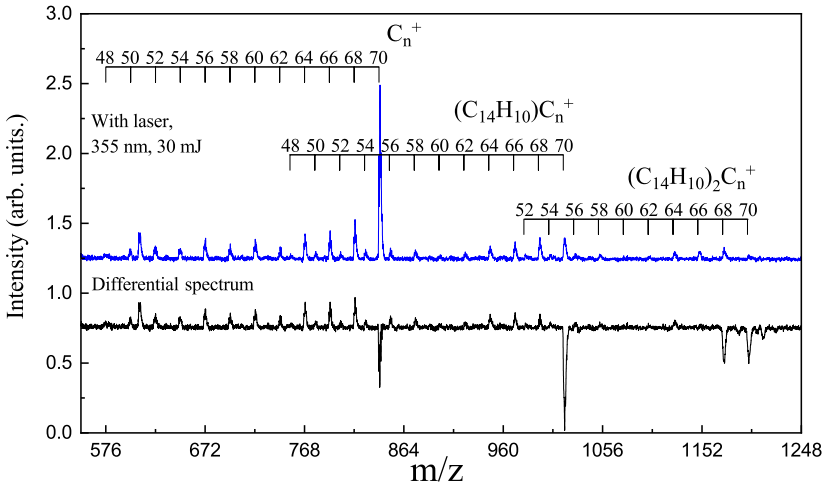

Fig. 4 The zoom-in mass spectrum of fullerene (C_{70})/anthracene cluster cations with laser irradiation and the differential spectrum in the range of m/z=552−1248.

($(C_{14}H_{10})C_{(70-2m)}^+$, $m = 2-11$) and bis-anthracene adducts ($(C_{14}H_{10})_2C_{(70-2m)}^+$, $m = 2-9$) were newly observed in current mass spectra (Fig. 3). Note that the laser wavelength (355 nm) used in these two studies is same. The newly observed smaller fullerene cations and their fullerene/anthracene cluster cations can be attributed to the higher energy (30 mJ pulse^{-1}) and longer irradiation time (1.6 s) used in the present experiment.

Irradiation UV photons upon the C_{70}^+/anthracene system, the generated smaller fullerene cations and their anthracene adducts all contain even numbers of carbon atoms. It is suggested that the successive C_2 loss is dominated the evolution process. After absorption of UV photons, fullerene/anthracene cluster cations ($(C_{14}H_{10})_mC_{68/70}^+$, $m = 1, 2$) dissociated into fullerene cations and anthracene (path 5). Then, the fullerene cations (including the free ones) underwent photo-fragmentation process (successive C_2 loss) and produced serials of smaller fullerene cations (path 6). Subsequently, these smaller fullerene cations reacted with anthracene molecules to form fullerene/anthracene cluster cations again (path 7 and 8). The photochemical pathways for the $C_{68/70}$/anthracene cluster cations are summarized as follows:

$$[(C_{14}H_{10})_{(1-2)}C_{68/70}]^+ \xrightarrow{h\nu} (C_{14}H_{10})_{(1-2)} + [C_{68/70}]^+ \quad (5)$$

$$[C_{68/70}]^+ \xrightarrow{h\nu} mC_2 + [C_{(70-2m)}]^+ \quad (6)$$

$$[C_{(70-2m)}]^+ + C_{14}H_{10} \longrightarrow [(C_{14}H_{10})C_{(70-2m)}]^+ \quad (7)$$

$$[(C_{14}H_{10})C_{(70-2m)}]^+ + C_{14}H_{10} \longrightarrow [(C_{14}H_{10})_2C_{(70-2m)}]^+ \quad (8)$$

The relative reactivity of fullerene cations can be derived from the intensity variations of fullerene cation-

s and their corresponding fullerene/anthracene cluster cations in the recorded mass spectra. To illustrate this, Figure 5(A) depicts the intensity ratios for (anthracene)fullerene cluster cations to fullerene cations recorded in the C_{60}/anthracene system and C_{70}/anthracene system individually. Figure 5(B) displays the intensity ratios for (anthracene)$_2$fullerene cluster cations to (anthracene)fullerene cluster cations recorded in the C_{60}/anthracene system and C_{70}/anthracene system individually. The peak intensity in the recorded mass spectra (Figs. 2 and 4) were used in the calculation. The intensity ratio calculated in this way is a reflection of the proportion that fullerene cations or (anthracene)fullerene cluster cations have reacted with free anthracene molecules. In other words, the larger the intensity ratio is, the higher reactivity the corresponding fullerene cation has. As shown in Figure 5(A), the intensity ratios for C_{60}/anthracene system are in a similar range with a central value of ≈0.7. The intensity ratios of C_{70}/anthracene system are in a similar range with a central value of ≈0.5 with the exception of C_{60}^+ whose value is about 0.1. Similar trends are found in Figure 5(B), the intensity ratio for $(C_{14}H_{10})C_{60}^+$ is of ≈ 0.1, which value is obvious smaller than the others. The significant lower values of the intensity ratios for C_{60}^+ and $(C_{14}H_{10})C_{60}^+$ illustrates that they have lower reactivity in addition reaction with anthracene molecules compared to the other fullerene cations. These results confirm the conclusion that C_{60}^+ has a lower reactivity reported in Ref. Zhen et al. (2019c) where the comparison is limited to C_{56}^+, C_{58}^+ and C_{60}^+ ions.

Although it is not as apparent as that of C_{60}^+ cation, there exists a slight variation of intensity ratio for other fullerene cations. As shown in Figure 5(A), the intensity ratio for C_{52}^+ appears as a local minimum in both C_{60}/anthracene and C_{70}/anthracene systems. Similar thing happens to C_{44}^+, C_{50}^+ and probably C_{56}^+. Considering that the mass spectra (Figs. 2 and 4) were recorded under an optimized and stable condition and that 200 average times were taken for each spectrum, the experimental factors (such as laser energy) that caused the intensity ratio variation should have been avoided. Moreover, the variation trends of intensity ratios are observed to be consistent on both C_{60}/anthracene and C_{70}/anthracene systems (Fig. 5(A)). If the slight variation is not caused by the experiment system errors, this indicates that, within the smaller fullerene cations (44–58 carbon atoms), C_{44}^+, C_{50}^+, C_{52}^+ and probably C_{56}^+ have relatively lower reactivity towards anthracene molecules. It should be mentioned that previous studies (Manolopoulos et al. 1991; Zimmerman et al. 1991; Rohlfing et al. 1984) have shown that the C_{44}, C_{50} and C_{56} are more stable than their neighbors. The recent theoretical work (Candian et al. 2019) addressed the stability of different isomers of C_{44}^+, C_{50}^+ and C_{56}^+. In their study, the stability is characterized in terms of the standard enthalpy of formation per CC bond, the HOMO−LUMO gap, and the energy required to eliminate a C_2 fragment. These studies (Manolopoulos et al. 1991; Zimmerman et al. 1991; Rohlfing et al. 1984; Candian et al. 2019) may explain the slight variation observed in present work.

4 ASTRONOMICAL IMPLICATIONS

The formation and evolution of neutral and charge state fullerenes in astronomical environments are of considerable interest, especially after the detection of C_{60} and C_{70} in the young planetary nebula Tc 1 via their IR emissions (Cami et al. 2010). To the best of our knowledge, it is still an open issue so far. In this work, we present the laboratory study of the formation and relative reactivity of fullerenes cations (C_{44}^+ to C_{70}^+). It is found that the higher laser energy and longer irradiation time are key factors to produce smaller fullerene cations. The increments of laser energy and irradiation time essentially increase photon number density. After absorption of UV photons, the fullerene cations undergo successive C_2 fragment loss dissociation which results in formation of smaller fullerene cations. This indicates that under the strong UV radiation environment like photon-dominated regions, the fullerene cations are probably driven to dissociate to smaller ones or even damage totally. That is to say the top-down evolution of fullerene cations is expected to be dominated in such regions. However, if the fullerene molecules are on the surface of dust grains, they may survive from the strong irradiation. The case in nebula Tc 1 may be a good example. By considering the temperature difference between the observed IR spectra and gas-phase environment in the nebula Tc 1, Cami et al. (2010) concluded that C_{60} and C_{70} are in direct contact with solid materials. The solid materials probably shield much UV radiation for the attached fullerenes. As a contrast, the gaseous fullerenes are exposed in the strong radiation environment, and are probably driven to smaller ones or damage. This may be a possible explanation for that no gaseous C_{60} and C_{70} are observed in Tc 1.

The second question addressed by this work is the relative reactivity of fullerene cations ($C_{(60-2n)}^+$, $n = 0-8$). The anthracene molecule is used as the reactant. It is found that the smaller fullerene cations show significantly high reactivity when compared to C_{60}^+. In the harsh ISM environment, anthracene molecules are not expected to survive. The most abundant interstellar PAHs are large condense ones (Ricca et al. 2012) which are highly reactive as anthracene. As is well known, the Diels–Alder

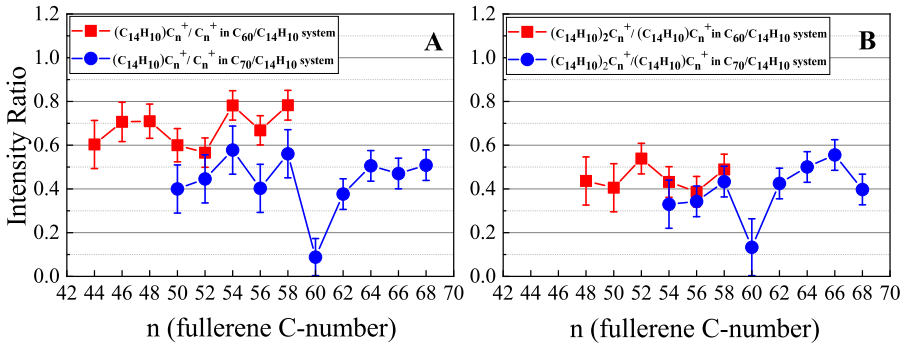

Fig. 5 Panel (A): the intensity ratio of formed (anthracene)fullerene cluster cations to fullerene cations in the irradiated spectrum: the red line is for the C_{60}/anthracene system; the blue line is for the C_{70}/anthracene system; Panel (B): the intensity ratio of formed (anthracene)$_2$fullerene cluster cations to (anthracene)fullerene cations in the irradiated spectrum: the red line is for the C_{60}/anthracene system; the blue line is for the C_{70}/anthracene system.

adduction is one of the routine ways when fullerene react with PAHs. In view of this point, other PAHs are expected to react with smaller fullerene cations in an efficient way like anthracene molecules. If the smaller fullerene and PAHs co-exist in the same astronomical region, they may react and form fullerene/PAHs adducts. These adducts may accumulate and contribute somewhat to the unidentified IR emission features. It is promising when noting the fact that C_{60}/anthracene adducts were shown to have strikingly similar spectral features to those from C_{60} (and C_{70}) fullerenes and other unidentified infrared emission features (García-Hernández et al. 2013).

5 CONCLUSIONS

The formation and relative reactivity of fullerene cations (from smaller to larger, $C_{44}{}^+$ to $C_{70}{}^+$) are studied in this work. It is found that the higher laser energy and longer irradiation time are key factors to produce the smaller fullerene cations such as $C_{(60-2n)}{}^+$, $n = 1 - 8$. When reacting with anthracene molecules, slightly different reactivity may exist within the smaller fullerene cations, if the experimental system errors are ruled out. Nevertheless, the smaller fullerene cations have significantly higher reactivity compared to $C_{60}{}^+$. A successive loss of C_2 fragments mechanism is suggested to account for the formation of smaller fullerene cations, which then undergo addition reaction with anthracene molecules. The results obtained here provide a growth route towards fullerene (from smaller to larger in size) derivatives based on PAH-related molecules in a bottom-up growth process and an insight for their photo-evolution behavior in the ISM. The results also suggest, when conditions are favorable, fullerene derivatives can form efficiently.

Acknowledgements This work is supported by the Fundamental Research Funds for the Central Universities, the National Natural Science Foundation of China (NSFC, Grant No. 11743004). We thank the referee for the very constructive and detailed comments which help improve this work a lot.

References

Allamandola, L. J., Tielens, A. G. G. M., & Barker, J. R. 1989, ApJS, 71, 733
Bernal, J. J., Haenecour, P., Howe, J., et al. 2019, ApJL, 883, L43
Berné, O., Cox, N. L. J., Mulas, G., & Joblin, C. 2017, A&A, 605, L1
Boersma, C., Rubin, R. H., & Allamandola, L. J. 2012, ApJ, 753, 168
Böhme, D. K. 2011, Phys. Chem. Chem. Phys., 13, 18253
Böhme, D. K. 2016, Philosophical Transactions of the Royal Society of London Series A, 374, 20150321
Briggs, J. B., & Miller, G. P. 2006, Comptes Rendus Chimie, 9, 916
Cami, J., Bernard-Salas, J., Peeters, E., & Malek, S. E. 2010, Science, 329, 1180
Campbell, E. K., Holz, M., Gerlich, D., & Maier, J. P. 2015, Nature, 523, 322
Candian, A., Gomes Rachid, M., MacIsaac, H., et al. 2019, MNRAS, 485, 1137
Cataldo, F., García-Hernández, D. A., & Manchado, A. 2014, Fullerene Nanotubes and Carbon Nanostructures, 22, 565
Cordiner, M. A., Linnartz, H., Cox, N. L. J., et al. 2019, ApJL, 875, L28
Evans, A., van Loon, J. T., Woodward, C. E., et al. 2012, MNRAS, 421, L92
García-Hernández, D. A., Cataldo, F., & Manchado, A. 2013, MNRAS, 434, 415
García-Hernández, D. A., Kameswara Rao, N., & Lambert, D. L. 2011, ApJ, 729, 126
Genzel, R., Lutz, D., Sturm, E., et al. 1998, ApJ, 498, 579

Jäger, C., Mutschke, H., Henning, T., & Huisken, F. 2008, ApJ, 689, 249
Kroto, H. W., Heath, J. R., Obrien, S. C., Curl, R. F., & Smalley, R. E. 1985, Nature, 318, 162
Li, A. 2020, Nature Astronomy, 4, 339
Lifshitz, C. 2000, International Journal of Mass Spectrometry, 198, 1
Linnartz, H., Cami, J., Cordiner, M., et al. 2020, Journal of Molecular Spectroscopy, 367, 111243
Manolopoulos, D. E., May, J. C., & Down, S. E. 1991, Chemical Physics Letters, 181, 105
Murata, Y., Kato, N., & Komatsu, K. 2001, The Journal of Organic Chemistry, 66, 7235
Omont, A. 2016, A&A, 590, A52
Peeters, E., Tielens, A. G. G. M., Allamand ola, L. J., & Wolfire, M. G. 2012, ApJ, 747, 44
Petrie, S., & Bohme, D. K. 2000, ApJ, 540, 869
Petrie, S., Javahery, G., Wang, J., & Bohme, D. K. 1992, Journal of the American Chemical Society, 114, 6268
Ricca, A., Bauschlicher, Charles W., J., Boersma, C., Tielens, A. G. G. M., & Allamand ola, L. J. 2012, ApJ, 754, 75
Roberts, K. R. G., Smith, K. T., & Sarre, P. J. 2012, MNRAS, 421, 3277
Rohlfing, E. A., Cox, D. M., & Kaldor, A. 1984, J. Chem. Phys., 81, 3322
Sellgren, K. 1984, ApJ, 277, 623
Sellgren, K., Werner, M. W., Ingalls, J. G., et al. 2010, ApJL, 722, L54
Tielens, A. G. G. M. 2008, ARA&A, 46, 289
Tielens, A. G. G. M. 2013, Reviews of Modern Physics, 85, 1021
Walker, G. A. H., Campbell, E. K., Maier, J. P., Bohlender, D., & Malo, L. 2016, ApJ, 831, 130
Zhang, Y., & Kwok, S. 2011, ApJ, 730, 126
Zhen, J., Castellanos, P., Paardekooper, D. M., Linnartz, H., & Tielens, A. G. G. M. 2014, ApJL, 797, L30
Zhen, J., Zhang, W., Yang, Y., & Zhu, Q. 2019a, MNRAS, 486, 3259
Zhen, J., Zhang, W., Yang, Y., & Zhu, Q. 2019b, MNRAS, 490, 3498
Zhen, J., Zhang, W., Yang, Y., Zhu, Q., & Tielens, A. G. G. M. 2019c, ApJ, 887, 70
Zimmerman, J. A., Eyler, J. R., Bach, S. B. H., & McElvany, S. W. 1991, J. Chem. Phys., 94, 3556